Fuel for hurricanes: bag-breakup fragmentation and sea spray giant droplets

Authors: Yu. Troitskaya[1]*, A. Kandaurov[1], O. Ermakova[1], D. Kozlov[1], D. Sergeev[1], S. Zilitinkevich[2,3]

Affiliations:

[1]Institute of Applied Physics, Nizhny Novgorod, Russia.

[2]Division of Atmospheric Sciences, University of Helsinki, Finland.

[3]Finnish Meteorological Institute, Helsinki, Finland.

*Correspondence to: yuliya@hydro.appl.sci-nnov.ru, sergej.zilitinkevich@fmi.fi.

The Beaufort scale based on the sea's appearance describes the criterion of the 'Force 8 wind' or gale as the beginning of breaking edges of wave-crests into the spindrift: the sea spray being torn by a violent wind. This observation suggests that the spindrift visualizes triggering of a new spray-generation regime with the threshold at the gale force wind. Here we indeed identify this new regime using high-speed video as the *bag-breakup* mode of fragmentation of liquid in gaseous flows known in a different context. This regime is characterized by inflating and consequent bursting of the short-lived objects, *bags*, comprising sail-like water films surrounded by massive liquid rims then fragmented to giant droplets with sizes exceeding 500 micrometers. From first principles of statistical physics we develop statistical description of these phenomena and show that at extreme winds the bag-breakup is the dominant spray-production mechanism. These findings provide a new basis for understanding and modeling of the air-sea exchange processes at extreme winds. The giant droplets by boosting the exchange processes explain significant increase of the air-sea thermal energy flux crucial for fast intensification of hurricanes. The bag-breakup also explains the hitherto enigmatic reduction of the surface drag coefficient in hurricanes.

Until recently, the sea spray, being a typical feature of the marine atmospheric boundary layer, remained the most uncertain factor among those controlling hurricanes and severe storms[1-3]. Due to enormous difficulties in field experiments at extreme winds, empirical estimates of the amount and sizes of droplets injected into the atmosphere from the ocean surface varied up to six orders of magnitude[4,5]. The very mechanisms of the spray production remained not fully understood[4,5]. The starting points for the present work have become the Beaufort scale based on the sea's appearance[6], where the criterion of the Force 8 wind or gale (17.2 – 20.7 m/s) is formulated as follows: "edges of (wave-)crests begin to break into spindrift". This observation assumes that the spindrift (or spume droplets, i.e. the sea spray torn by a violent wind from wave crests) is a visual manifestation of a new spray-generation regime which activates at the gale force wind.

We identify this spray-generating regime in experiments specially designed to investigate how extremely strong winds tear off spume droplets from wave crests. Employing high-speed video-filming enabled us to classify the spray-generating events and to quantify the efficiency of the disclosed mechanisms. Experiments were carried out in high-speed wind-wave flume[7] (see details of the experimental setup in Methods and Supplementary Materials, Section A1). We characterize the near-water boundary layer by the friction velocity, u_*, defined via vertical turbulent shear stress: $F_M = \rho_{air} u_*^2$, where ρ_{air} is the air density. In our experiments friction velocity, u_*, varied between 0.8 and 1.51 m/s. According to known empirical relationship[8], in

the field conditions these values correspond to the wind speeds at the reference height 10m, U_{10}, between 18.4 (Beaufort number 8)[6] and 35 m/s (Category 1 hurricane)[9].

Basing on video-filming done at the rates up to 10000 fps we formulate the following classification of spray-generating mechanisms.

1) Breaking projection (Fig.1A and video S1)

Small "projections"[10] develop mainly at crests of breaking waves and break into a few droplets with 1-2 millimetre diameters.

2) Underwater bubble-bursting (Fig.1B and video S2)

Underwater bubbles forming at crests of breaking waves burst into droplets when reach the water surface[11]. This mechanism is usually considered as a major one responsible for generation of marine aerosol[11]. Contrastingly, our video-filming has revealed its surprising inefficiency: only about 5% of the observed underwater bubbles reach water surface and burst to produce droplets.

3) Bag-breakup (Fig.1C and video S3)

Typical event of this type starts with a small-scale elevation of the water surface, which then develops into a bag, inflates into a water film bordered by thicker rim, and finally blows up. In engineering fluid dynamics[12] this phenomenon is known as the bag-breakup mode of liquid fragmentation in gaseous flows. Recently an evidence of the bag-breakup spray generation in laboratory flume was also reported[13].

Comparative efficiency of the above mechanisms quantified by processing about 2.3 million video-frames (see Supplementary Materials, Section A1 for details of the algorithm) is illustrated in Fig. 1D, where each mechanism is characterized by the specific number of events arisen per unit time over unit area as dependent on the friction velocity, u_*. At $u_* < 1$ m/s the three mechanisms are almost equally efficient, but at $u_* > 1$ m/s the number of bursting bubbles lags essentially behind the numbers of projections and bags. Moreover, breaking projections yield up to 3 droplets per event; so the bag-breakups, yielding about one hundred of droplets per event, become absolutely dominant. Note, that in our experiments, the threshold of the bag-breakup regime was $u_* \approx 0.9$ m/s, which corresponds to $U_{10} \approx 20$ m/s [8] that is to the Beaufort Number 8[6] (see Fig.1D) which, in turn, is precisely the wind force, when the "spindrift" first appears.

To determine specific number, N_L, of the bag-breakup events versus the wind force or friction velocity, we employ phenomenological statistical-physics approach using the Gibbs method[14] for description of statistics of the energy states of a "quasi-thermodynamic system" comprising wave crests that can be potentially transformed into "bags" and then atomized into spray when its energy exceeds a certain threshold required for activation of the bag-breakup regime. Derivation of the function $N_L(u_*)$ is given in Supplementary Materials, Section A2. Its good fit to experimental data is illustrated in Fig.1D.

Processing video-frame consequences allowed us to determine the distribution of bags in radii, R, and life-times, τ. Mean values of these parameters, roughly estimated as $\langle R \rangle \sim 10^{-2}$ m and $\langle \tau \rangle \sim 10^{-2}$-$10^{-1}$ s, generally decrease with increasing wind speed (Eq. S5, S7 in Supplementary Materials, Section A2). This has strong effect on the surface stress and the drag coefficient.

Knowing statistics of bags, we derive the bag-breakup "sea spray generation function" (SSGF) defined as the volume of droplets of radius r produced from the unit area of water surface in unit time due to the dominant bag-breakup mechanism. As seen in Fig.1C, bags generate spray in two ways:

- rupturing the film of inflated bag (Fig. 1C, 6.8 ms), which yields film-droplets with average radius ~100 μm,
- fragmenting the rim, which preserves for a while after the bag's blow up (Fig. 1C, 11.6 ms), thus yielding rim-droplets with average radius ~1000 μm.

Herewith, the sizes of droplets are prescribed by the sizes of bags.

The resulted SSGF (Fig. 2A,B) has two peaks corresponding to the film- and rim-droplets, respectively (see derivation in Supplementary Materials, Section A3). The rim-droplet peak at r = 500-1000 μm is the distinctive feature of the bag-breakup spray generation mechanism. Such giant droplets torn off the wave crests are obtained in topical laboratory experiments reproducing the hurricanes conditions[13,15].

We have also verified our bag-breakup sea spray generation function (SSGF) against data obtained in field[16-18] (Fig.2B). To convert the laboratory SSGF to the field conditions, we use well-documented[16] empirical dependence of SSGF on fetch (the distance which the wave field has passed under the action of wind). For the typical of hurricanes rotating and displacing wind fields, fetch is a poorly determined parameter. In our analyses we characterize fetch by the wave-age parameter, $\Omega = U_{10}/c_p$, where c_p is the phase speed of the dominant surface waves. Direct measurements in the hurricane conditions[19] yielded Ω = 2-3. Fig.2B shows quite good correspondence between our "theoretical+lab-experiment SSGF" and "empirical SSGFs"[15-17] in the radii interval 30μ < r < 300μm. It is by no means surprising that the giant rim droplets with r > 300mm are missed in[16-18], where SSGFs were derived through extrapolation of data obtained at winds below 20 m/s[20], when the bag-breakup mechanism was not activated.

The bags and giant droplets, the "hallmark" of the bag-breakup mechanism, turn out to make significant contribution to both heat energy supply from the ocean and mechanical dissipation in the atmospheric boundary layer, i.e. factors responsible for development and maintenance of hurricanes[21].

In particular, the effect of bags and giant droplets can explain the effective smoothing of the water surface equivalent to surface drag reduction at hurricane winds disclosed in meteorological[22-24] and oceanographic[25] observations. Indeed, the contribution of the bag-breakup to the momentum flux consists of the two parts:

- the droplet-stress, F_{Md}, equal to the amount of momentum acquired by droplets in the course of their production (basically attributed to large droplets; see Fig.3A),
- the bag-stress, F_{Mb}, provided by bags – "micro sails" with typical sizes about 1 cm, which make obstacles to the near-water airflow.

Derivation of F_{Md} and F_{Mb} are given in Supplementary Materials, Section A4. Both bag-stress and droplets-stress are leveling off at high winds (see Fig.3B) due to the following counteracting impacts of the increasing wind speed: increasing number of bags and more spray, and weakening their individual contributions to the momentum flux due to decreasing sizes and life-times of bags. The revealed saturation of the momentum flux just prescribes the seemingly paradoxical peaking of the surface drag coefficient $C_D = F_M / U_{10}^2$ (Fig.3C). For completeness, we take into account in this Figure the effect of suspended droplets on the static stability in the near-surface air flow, which creates the stable stratification and thus slightly reduces turbulence in the marine atmospheric boundary layer[3,26](see details in Supplementary Materials, Section A5).

The contribution from spray to the thermal energy supply from ocean to atmosphere through evaporation (quantified by the vertical flux of moist enthalpy, H_k) is provided by large enough droplets, which cool down below the ambient air temperature (due to evaporation of only small fractions) of their volumes and then re-enter to water[1]. Fig. 3D confirms dominant contribution to this process of the giant rim-droplets, especially at winds exceeding 35 m/s when the contribution of spray exceeds the near-surface turbulent heat flux (see Fig.3E). As a result, the enthalpy exchange coefficient $C_k = H_k \big/ \left(\rho_a U_{10} \left(k_{10} - k_s\right)\right)$ (where k_{10} and k_s are the specific moist enthalpy at the reference height 10 m and at the sea level, respectively) increases with strengthening wind (Fig.3F) (see details in Supplementary Materials, Section A6). Consequently the ratio of the exchange coefficients C_k/C_D increases and at 35-40 m/s wind exceeds 0.75, which is just the renown threshold for development of tropical cyclones[21] (Fig.4).

Our analyses has revealed that the dominant spray-generation mechanism in extreme winds roots in specific instability at the air-water interface known in engineering fluid mechanics as the bag-breakup fragmentation. Coincidence of the activation thresholds enables us to identify the

bag-breakup with the spindrift – the signature of the force 8 wind of the Beaufort scale based on the sea's appearance[6]. In view of this finding, it seems natural to assume that the criterion of the Force 11 wind, namely, "the edges of the wave crests are blown into froth"[6] is nothing but a manifestation of another yet unknown feature of the air-sea coupling at extreme winds.

Methods

The experiments were carried out in the wind-wave flume of Large Thermally Stratified Tank of IAP RAS. The airflow channel with the cross-section of 0.4×0.4 m over the water surface had the length of 10 m. The tank was filled with fresh water, with temperature ranging during experiments from 15 to 20°C. The measured value of the surface tension was $\sigma = (7.0\pm0.15)\cdot10^{-2}$ N/m. The facility and parameters of air flow and surface waves are described in details in[7].

Measurements were carried out in two working sections spaced 7 and 8 m from the outlet of the fan. Video filming of the air-water interface was done by the high-speed digital camera NAC Memrecam HX-3 from two different angles: side view – using the vertical matte screen and surface LED 300W lights (horizontal shadow method); and top view – using underwater illumination (vertical shadow method).

The side view filming gave us overall views of spray-generating phenomena. The optical axis of the camera lens was located 5 cm above the water surface and directed horizontally. The distance from the camera to the shooting area was 65 cm. A LED spotlight was mounted at the side of the channel section 8 at the distance 50 cm from the wall and the height less than 5 cm from the water surface. A matte screen was placed on the side wall of the channel opposite to the camera. We used the lenses with focal lengths 50 and 85 mm with resolution 55-55-119 μm/px. The recording rate was 10000 fps. For wind speeds from 22.2 to 39.5 m/s we obtained less than a second long detailed records of the surface features, while working with the camera records we only selected parts of the records containing the spray generation. Typical images of events leading to the spray generation are shown in Fig. 1(A-C) and movies S1-S3.

To obtain statistical data for the events on the surface leading to spray generation, video-filming was done using the vertical shadow method. Filming was conducted through the transparent top wall of the channel section. Camera was mounted vertically at the distance 207 cm from the water surface. Video-filming was carried out at rates 4500 and 10000 fps with the scales 256 and 124 μm/px, respectively, in the wide range of wind speeds: 22.2-39.5 m/s.

Statistical data for the events on the surface leading to the spray generation was retrieved from video-filming using specially developed software allowed for semi-automatic registering of the events leading to spray generation: breaking projections, bursting underwater bubbles, and "bag-breakup". The software provided convenient way to browse through recordings at slow speed of frame-by-frame, to find the features of interest and to mark them. Markers were manually added to the image sequences using computer mouse. In total, 69 video-films containing about 33000 frames each were processed to get the statistics.

Scheme of the experimental setup and details of the data processing algorithm are given in Supplementary Materials, Section A1. The theoretical derivation of the statistics of bag-breakup events, equation for the "bag-breakup" spray generation function and estimations of contributions of droplets to heat and momentum fluxes in the storm atmospheric boundary layer are presented in Supplementary Materials, Sections A2-A6.

References:

1. Andreas, E. L. & Emanuel, K. A. Effects of Sea Spray on Tropical Cyclone Intensity. *J. Atmos. Sci.* **58,** 3741–3751 (2001).

2. Andreas, E. L. Fallacies of the Enthalpy Transfer Coefficient over the Ocean in High Winds. *J. Atmos. Sci.* **68,** 1435–1445 (2011).

3. Bao, J.-W., Fairall, C. W., Michelson, S. A. & Bianco, L. Parameterizations of Sea-Spray Impact on the Air–Sea Momentum and Heat Fluxes. *Mon. Weather Rev.* **139,** 3781–3797 (2011).

4. Massel, S.R. *Ocean waves breaking and marine aerosol fluxes*. p. 232 (Springer, New York, 2007).

5. Andreas, E. L. in *Atmosphere-Ocean Interactions Volume 1* (ed. Perrie, W.) 1–46 (WIT Press, Billerica, Mass, 2002).

6. National Meteorological Library and Archive Fact sheet 6 — The Beaufort Scale.

7. Troitskaya, Y. I. *et al.* Laboratory and theoretical modeling of air-sea momentum transfer under severe wind conditions. *J. Geophys. Res. Ocean.* **117,** C00J21 (2012).

8. Foreman, R. J. & Emeis, S. Revisiting the Definition of the Drag Coefficient in the Marine Atmospheric Boundary Layer. *J. Phys. Oceanogr.* **40,** 2325–2332 (2010).

9. Saffir-Simpson Hurricane Wind Scale, http://www.nhc.noaa.gov/aboutsshws.php

10. Koga, M. Direct production of droplets from breaking wind-waves —its observation by a multi-colored overlapping exposure photographing technique. *Tellus* **33,** 552–563 (1981).

11. Wu, J. Evidence of sea spray produced by bursting bubbles. *Science* **212,** 324–326 (1981).

12. Gelfand, B.E. Droplet breakup phenomena in flows with velocity lag. Prog. Energ. Combust. Sci. **22**, 201–265 (1996).

13. Veron, F., Hopkins, C., Harrison, E. L. & Mueller, J. A. Sea spray spume droplet production in high wind speeds. *Geophys. Res. Lett.* **39,** L16602 (2012).

14. Gibbs, J. W. *Elementary Principles in Statistical Mechanics*. (Charles Scribner's Sons, 1902).

15. Iida, N., Toba, Y. & Chaen, M. A new expression for the production rate of sea water droplets on the sea surface. *J. Oceanogr.* **48,** 439–460 (1992).

16. Zhao, D., Toba, Y., Sugioka, K. & Komori, S. New sea spray generation function for spume droplets. *J. Geophys. Res. Ocean.* **111,** C02007 (2006).

17. Fairall, C. W., Kepert, J. D. & Holland, G. J. The effect of sea spray on surface energy transports over the ocean. *Glob. Atmos. Ocean Syst.* **2,** 121–142 (1994).

18. Andreas, E. L. A New Sea Spray Generation Function for Wind Speeds up to 32 m s−1. *J. Phys. Oceanogr.* **28,** 2175–2184 (1998).

19. Wright, C. W. *et al.* Hurricane Directional Wave Spectrum Spatial Variation in the Open Ocean. *J. Phys. Oceanogr.* **31,** 2472–2488 (2001).

20. Andreas, E. L. Sea spray and the turbulent air–sea heat fluxes. *J. Geophys. Res.* **97,** 11 429–11 441 (1992).

21. Emanuel, K. A. Sensitivity of Tropical Cyclones to Surface Exchange Coefficients and a Revised Steady-State Model incorporating Eye Dynamics. *J. Atmos. Sci.* **52,** 3969–3976 (1995).

22. Powell, M. D., Vickery, P. J. & Reinhold, T. A. Reduced drag coefficient for high wind speeds in tropical cyclones. *Nature* **422,** 279–283 (2003).

23. Holthuijsen, L. H., Powell, M. D. & Pietrzak, J. D. Wind and waves in extreme hurricanes. *J. Geophys. Res. Ocean.* **117,** C09003 (2012).

24. Donelan, M. A., et al. On the limiting aerodynamic roughness of the ocean in very strong winds. *Geophys. Res. Lett.*, **31**, L18306 (2004).

25. Jarosz, E., Mitchell, D. A., Wang, D. W. & Teague, W. J. Bottom-Up Determination of Air-Sea Momentum Exchange Under a Major Tropical Cyclone. *Science* **315,** 1707–1709 (2007).

26. Kudryavtsev, V. N. On the effect of sea drops on the atmospheric boundary layer. *J. Geophys. Res.* **111,** C07020 (2006).

27. Richter, D. H., Bohac, R. & Stern, D. P. An assessment of the flux profile method for determining air-sea momentum and enthalpy fluxes from dropsonde data in tropical cyclones. *J. Atmos. Sci.* (2016). doi: 10.1175/JAS-D-15-0331.1 (in press).

28. Bell, M. M., Montgomery, M. T. & Emanuel, K. A. Air-Sea Enthalpy and Momentum Exchange at Major Hurricane Wind Speeds Observed during CBLAST. *J. Atmos. Sci.* **69,** 3197–3222 (2012).

29. Black, P. G. *et al.* Air-sea exchange in hurricanes: Synthesis of observations from the Coupled Boundary Layer Air-Sea Transfer experiment. *Bull. Am. Meteorol. Soc.* **88,** 357–374 (2007).

Figure Legends

Fig. 1. Mechanisms of spray generation: A – breaking projection (top view); B – rupture of large bubble (side view); C – formation and rupture of bag (side view); D – number of local spray generating phenomena per unit time per unit area versus the friction velocity u_* and the Beaufort number: blue squares – bursts of floating bubbles, cyan squares – projections, red circles – bag breakup; red solid curve – our formulation based on the Gibbs or canonical distribution (Eq.S3 in Supplementary Materials, Section A2).

Fig. 2. (A) Comparison of our bag-breakup sea spray generation function (SSGF) as a volume flux (red lines) with empirical SSGFs[16] for laboratory conditions (blue lines); friction velocity u_* varies between 1 and 1.5 m/s with increment 0.1 m/s. (B) Comparison of our SSGF with empirical SSGFs for field conditions[16-18] at U_{10}=30 m/s (top) and U_{10}=35 m/s (bottom).

Fig. 3. Size distribution of the contribution from droplets to (A) the of momentum flux, P, and (D) the enthalpy flux, E; wind speed U_{10} varies between 20 and 60 m/s with increment 2 m/s. (B) Contributions to the surface stress caused by bags, droplets and direct turbulent transfer versus 10-m wind speed, U_{10}, for the wave-age parameter, Ω, from 2 to 3. (C) The surface drag coefficient, C_D, versus, U_{10} after our stress model for Ω between 2.5 and 3.5. Dashed red curve shows C_D from[8]. Experimental data: dark blue squares, diamonds, triangles and circles[22], crosses[23], asterisks[28], close circles[27], blue dots[25]; blue solid curve and dashed curves are the polynomial best fit and 95% confident interval of data[25]; solid red curves show our bag stress model for Ω between 2.5 and 3.5. (E) Contributions to the enthalpy flux from droplets and from direct turbulent transfer versus 10-m wind speed, U_{10}, for the wave-age parameter, Ω, varying from 2.5 to 3.5. (F) The enthalpy transfer coefficient, C_k, versus, U_{10} from our stress model for Ω varying from 2.5 to 3.5; experimental data: dark blue triangles[29], close circles[27].The hurricane thermodynamics parameters are: air temperature 25°C, water temperature 27.5°C, relative humidity 96%.

Fig.4. The ratio of the enthalpy and drag coefficients from our model versus 10-m wind speed, U_{10}, for the wave-age parameter, Ω, varying from 2.5 to 3.5. Dashed red line denotes the level 0.75 – the threshold for the tropical cyclone development according to[21]. Experimental data: dark blue triangles[29], close circles[27].

Supplementary Materials:

Supplementary Text

Figures S1-S5

Movies S1-S3

External Database S1

References[30-41]

Acknowledgments: Data reported in this paper are available in Supplementary Materials (the zipped archive S1.zip). This work has been supported by the Russian Science Foundation project No.14-17-00667), Seventh Framework Programme (project PIRSES-GA-2013-612610) and Russian Foundation for Basic Research projects (16-05-00839, 14-05-91767). SZ additionally acknowledges support from the Academy of Finland project ABBA No. 280700. The authors thank Professors Markku Kulmala, Tuukka Petaja and Victor Shrira who have read the manuscript and given valuable comments.

Author contributions:

Y.T., D.S. and S.Z. had the original idea, A.K. and D.S. designed and performed experiments. A.K. developed software for analysis of optical images and O.E. performed data evaluation. Y.T., S.Z. and D.K. made the theoretical derivation of the statistics of bag-breakup events; equation for the "bag-breakup" spray generation function and estimated contributions of droplets to heat and momentum fluxes in the storm atmospheric boundary layer. Y.T. and S.Z. wrote the manuscript. All authors discussed the results and commented on the paper.

Competing financial interests:

The authors declare no competing financial interests.

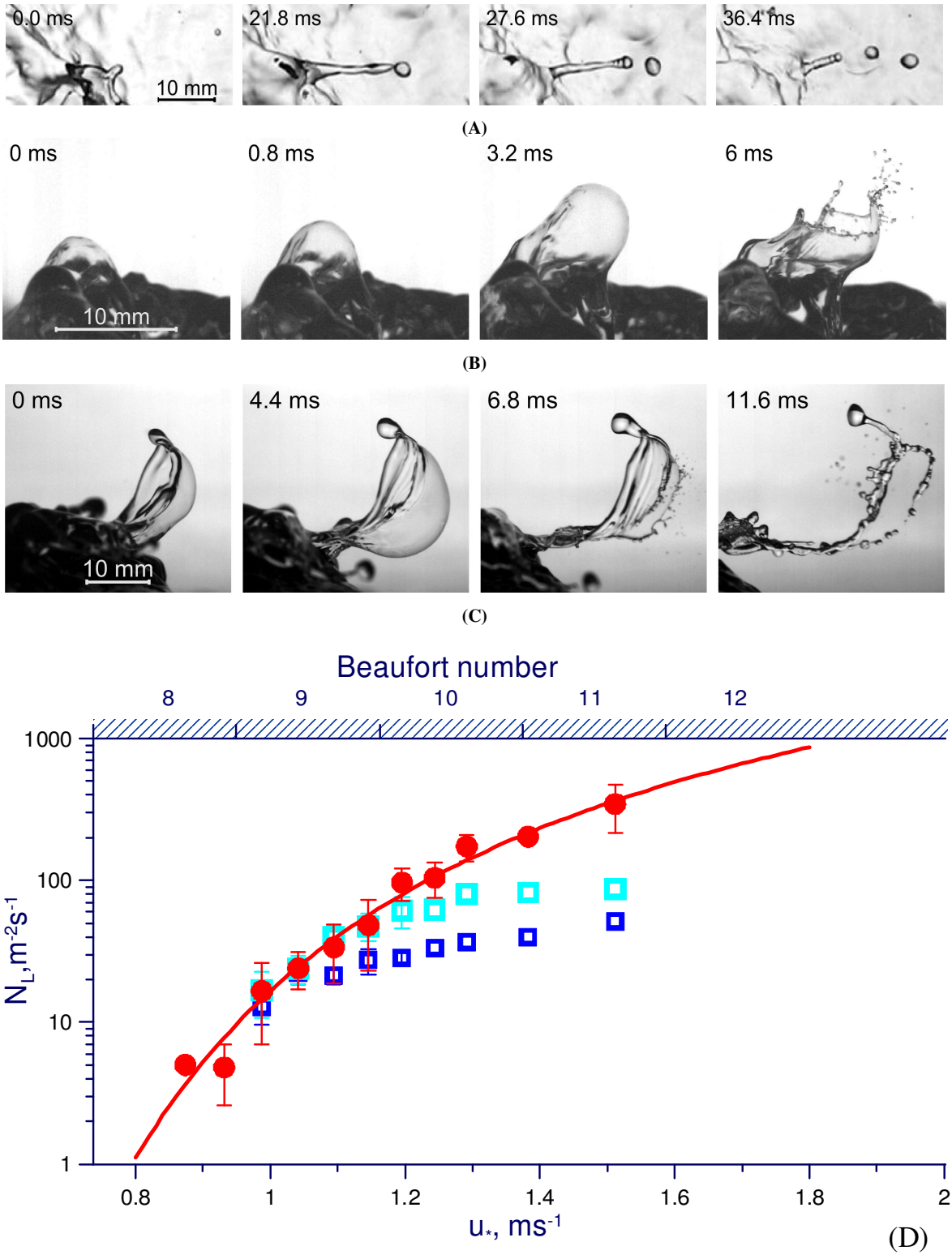

Fig. 1. Mechanisms of spray generation: A – breaking projection (top view); B – rupture of large bubble (side view); C – formation and rupture of bag (side view); D – number of local spray generating phenomena per unit time per unit area versus the friction velocity u_* and the Beaufort number: blue squares – bursts of floating bubbles, cyan squares – projections, red circles – bag breakup; red solid curve – our formulation based on the Gibbs or canonical distribution (Eq.S3 in Supplementary Materials, Section A2).

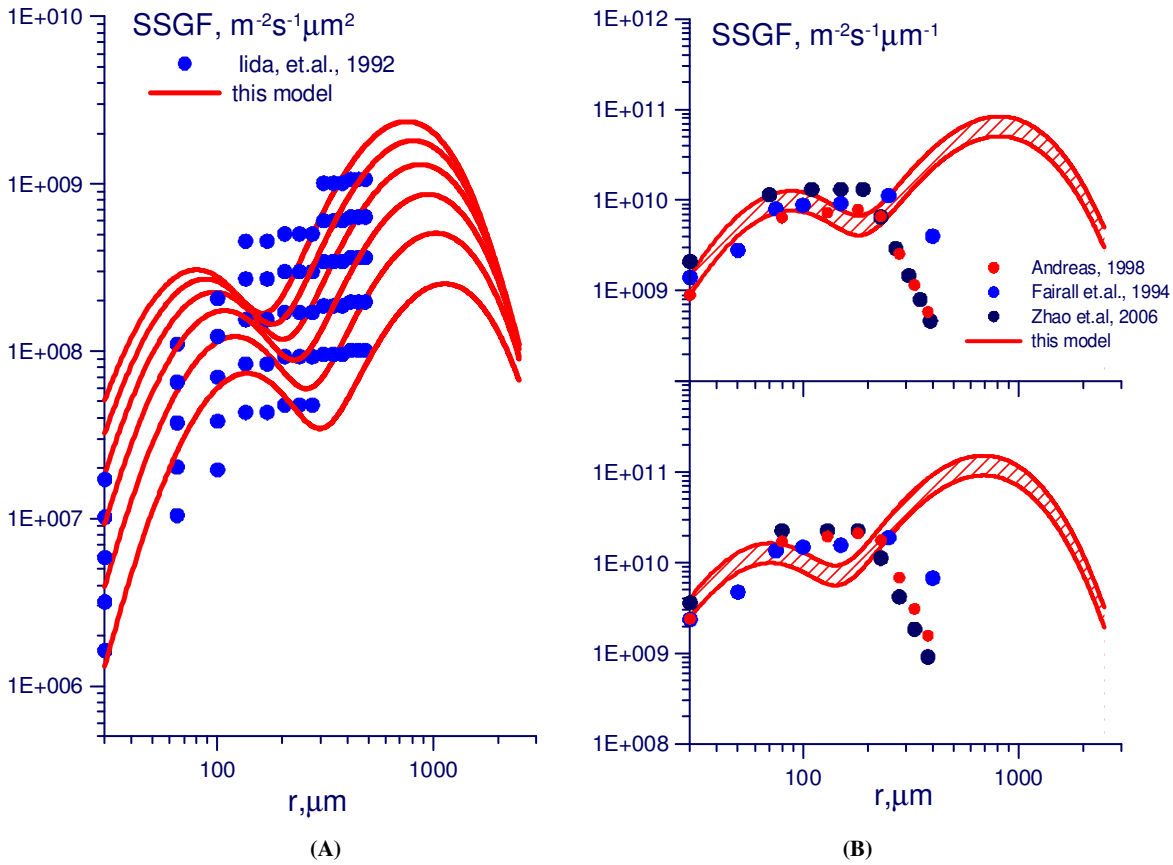

Fig. 2. (A) Comparison of our bag-breakup sea spray generation function (SSGF) as a volume flux (red lines) with empirical SSGFs[16] for laboratory conditions (blue lines); friction velocity u_* varies between 1 and 1.5 m/s with increment 0.1 m/s. (B) Comparison of our SSGF with empirical SSGFs for field conditions[16-18] at U_{10}=30 m/s (top) and U_{10}=35 m/s (bottom).

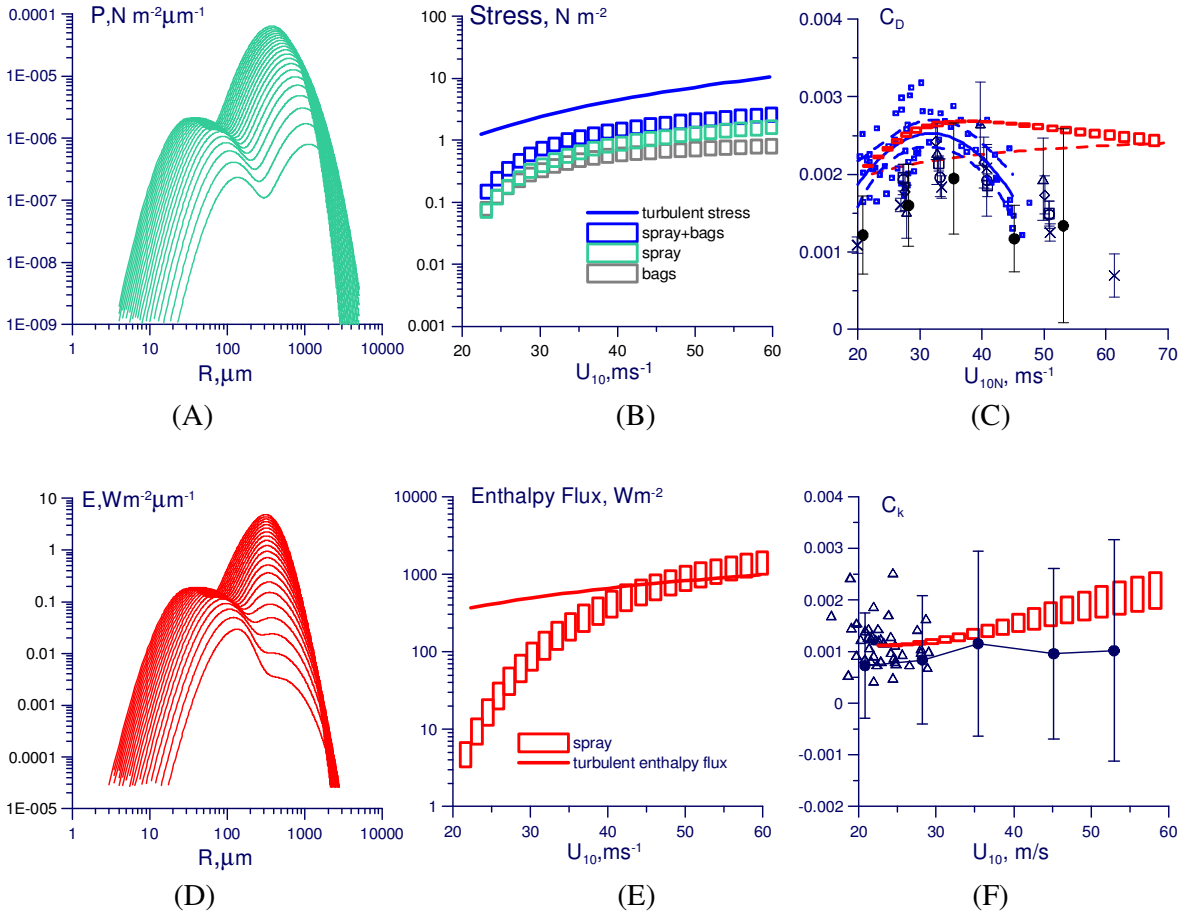

Fig. 3. Size distribution of the contribution from droplets to (A) the of momentum flux, P, and (D) the enthalpy flux, E; wind speed U_{10} varies between 20 and 60 m/s with increment 2 m/s. (B) Contributions to the surface stress caused by bags, droplets and direct turbulent transfer versus 10-m wind speed, U_{10}, for the wave-age parameter, Ω, from 2 to 3. (C) The surface drag coefficient, C_D, versus, U_{10} after our stress model for Ω between 2.5 and 3.5. Dashed red curve shows C_D from[8]. Experimental data: dark blue squares, diamonds, triangles and circles[22], crosses[24], asterisks[28], close circles[27], blue dots[25]; blue solid curve and dashed curves are the polynomial best fit and 95% confident interval of data[25]; solid red curves show our bag stress model for Ω between 2.5 and 3.5. (E) Contributions to the enthalpy flux from droplets and from direct turbulent transfer versus 10-m wind speed, U_{10}, for the wave-age parameter, Ω, varying from 2.5 to 3.5. (F) The enthalpy transfer coefficient, C_k, versus, U_{10} from our stress model for Ω varying from 2.5 to 3.5; experimental data: dark blue triangles[29], close circles[27].The hurricane thermodynamics parameters are: air temperature 25°C, water temperature 27.5°C, relative humidity 96%.

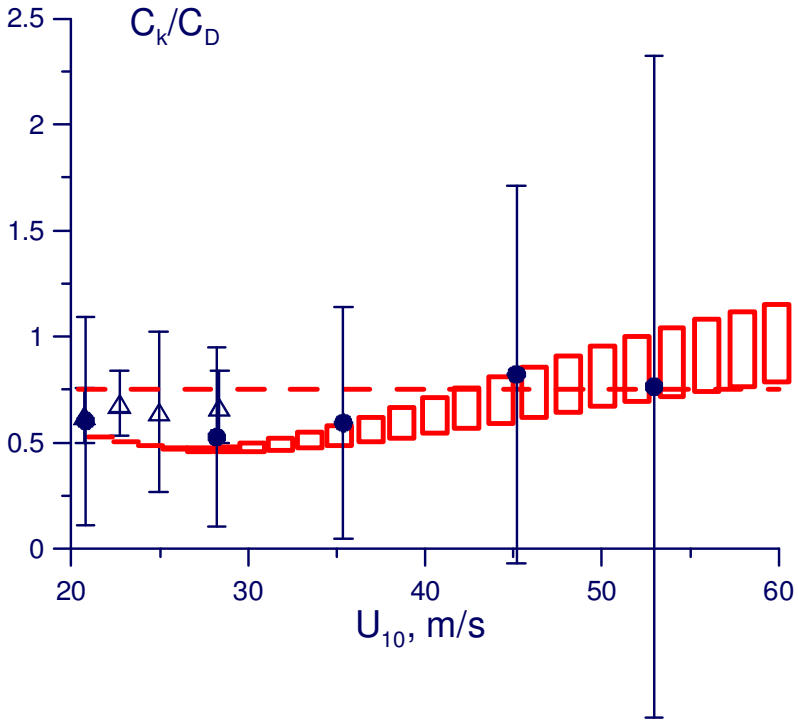

Fig.4. The ratio of the enthalpy and drag coefficients from our model versus 10-m wind speed, U_{10}, for the wave-age parameter, Ω, varying from 2.5 to 3.5. Dashed red line denotes the level 0.75 – the threshold for the tropical cyclone development according to[21]. Experimental data: dark blue triangles[29], close circles[27].